International Journal of Polymeric Materials, 57:1104–1118, 2008

ISSN: 0091-4037 print/1563-535X online
DOI: 10.1080/00914030802341679

Taylor & Francis
Taylor & Francis Group

Permeation of Oxygen and Nitrogen Gases through Poly(ethylene-co-vinyl acetate) Membranes

S. Anil Kumar,[1] M. N. Muralidharan,[1,2] M. G. Kumaran,[3] Abi Santhosh Aprem,[4] and Sabu Thomas[5]
[1]Department of Chemistry N. S. S. College, Ottapalam, Palakkad, Kerala, India
[2]Department of Polymer Science and Rubber Technology, Cochin University of Science and Technology, Kochi, Kerala, India
[3]Rubber Research Institute of India, Kottayam, Kerala, India
[4]Hindustan Latex Limited, Thiruvananthapuram, Kerala, India
[5]School of Chemical Sciences, Mahatma Gandhi University, Kottayam, Kerala, India

The transport of oxygen and nitrogen gases through uncrosslinked and crosslinked poly(ethylene-co-vinyl acetate) membranes has been analyzed. Poly(ethylene-co-vinyl acetate) was crosslinked by dicumyl peroxide and benzoyl peroxide. Neat sample showed a lower permeation coefficient due to the crystalline nature. The crystalline nature was supported by X-ray diffraction analysis. The difference in the permeation behavior of the two crosslinked samples was correlated with crosslink density. Crosslink density was calculated using equilibrium sorption method. Differential scanning calorimetry analysis also supports the different permeation behavior of the crosslinked samples. The O_2/N_2 selectivity of the membranes was estimated. The influence of the crosslink density and size of penetrants on permeation were analyzed. The effect of free volume on the gas barrier properties was investigated by positron annihilation lifetime spectroscopy.

Keywords: gases, permeation, poly(ethylene vinyl acetate)

INTRODUCTION

Polymer membranes are considered a viable and effective technology for the separation of gaseous mixtures in industrial applications due

Received 16 June 2008; in final form 23 June 2008.
Address correspondence to M. N. Muralidharan, Department of Polymer Science and Rubber Technology, Cochin University of Science and Technology, Kochi – 682 022, Kerala, India. E-mail: anugraha_anil@yahoo.co.in

to their high separation efficiency, simple operation, and low capital and operating costs. The performance of the membrane strongly depends on the permeability and selectivity of the membrane. Membrane with higher permeability leads to higher productivity and lower capital costs, whereas membrane with higher selectivity leads to more efficient separation, higher recovery and lower power costs. Indeed, membranes that simultaneously possess high values of selectivity and permeability would lead to the most economical gas separation processes. Hence, numerous studies and efforts were centered on the development of high performance membranes for the gas separation process [1–11].

The transport of gases through a membrane depends on various factors such as permeant size, shape and phase, polymer molecular weight, functional groups, density and polymer structure, crosslinking, and crystallinity [12]. Paul and coworkers [13,14] have investigated the relationship between gas transport and polymer structure. The introduction of functional groups in the polymer chain can alter the permeability and selectivity due to variation in the polarity and free volume within the polymer [15]. The selective transport of gases through polymeric membranes has been reviewed by Aminabhavi and coworkers [16]. Van Amerongen [17] studied the permeability of various gases through elastomers. Thomas and coworkers [18,19] investigated the gas transport properties of various blends. They concluded that permeation is a process in which gas molecules dissolve in the elastomer on one side of a membrane, diffuse to the other side and then evaporate. The rate of diffusion in a given polymer is found to be related chiefly to the size of the gas molecule. It was observed that the presence of polar or methyl groups in the polymer molecule reduces the permeability of a given gas. In the case of permeant gases such as nitrogen, oxygen and hydrogen the permeability depends on the nature of the gas, the membrane material, temperature and pressure. Chen et al. [20] reported the sorption and transport mechanism of gases in polycarbonate membranes (PC). A better understanding of the mechanism of gas diffusion in polymers is highly desirable in order to achieve significant improvements in the membrane-assisted transport process. In this paper, the permeation characteristics of uncrosslinked and crosslinked poly(ethylene-co-vinyl acetate) membranes are presented. The gas permeability coefficient and separation factors have been measured. Also, the effect of crosslinker loading on gas permeability was studied. The influence of free volume on gas permeation was analyzed using positron annihilation lifetime spectroscopic analysis (PALS).

EXPERIMENTAL

Materials

Poly(ethylene-co-vinyl acetate) EVA (Pilene, 1802) used was supplied by Polyolefin Industries Limited, Chennai, India. The basic characteristics of the copolymer are given in Table 1. The crosslinking agents used were dicumyl peroxide (DCP) and benzoyl peroxide (BP).

Membrane Preparation

Membranes of EVA were fabricated by using two crosslinking agents, namely DCP and BP. Unmodified EVA membranes were also prepared. The unmodified membranes are represented as D_0. EVA granules were sheeted out on a two-roll mixing mill with a friction ratio 1:1.4. The sheeted out stock was pressed on a hydraulic press at 170°C and under a load of 24.5×10^3 N. The modified membranes were prepared using BP and DCP. The mixing was done on a two-roll mixing mill as before. The cure behavior was studied with a Geottfert rheometer. The samples were then cured up to their optimum cure time. DCP-modified membranes were cured at 170°C and under a load of 24.5×10^3 N (represented as D). BP-modified membrane was cured at 120°C and under a load of 24.5×10^3 N (represented as B_1). Membranes with different loading of DCP were also prepared. DCP-modified membranes are designated as D_1, D_2, D_4, D_6 and D_8 according to the DCP content where the subscript numbers represent the grams of DCP used per 100 grams of the polymer. Similarly BP-modified membrane is represented as B_1, according to the BP content.

TABLE 1 Details of Material Used

Material	Properties		Source
Poly(ethylene-co-vinyl acetate)	Melt flow index (kg/600s)	2×10^{-3}	PIL Chennai India
	Density (kg/m^3)	0.937×10^3	
	Vicat softening point (°C)	59.0	
	Vinyl acetate (%)	18.0	
	Intrinsic viscosity (m^3/kg)	0.017	

Gas Permeation Studies

The measurements were done using the ATS FAAR gas permeability tester in manometric method in accordance with the ASTM standard D1434. The permeabilities of O_2 and N_2 gases through EVA membranes were tested at various pressures.

Crosslink Density Measurements

The EVA samples for sorption experiments (ASTM D-471) were punched out in circular shapes of 19 mm diameter from tensile sheets and dried in a vacuum desiccator over anhydrous $CaCl_2$ at room temperature for about 24 h. The original weight and thickness of the samples were measured. They were then immersed in benzene (15–20 ml) in closed diffusion bottles, and kept at constant temperature in an air oven until equilibrium was attained. The samples were removed from the bottles, dried for 5–10 s between filter papers to remove the excess solvent on their surface and weighed instantly in an electronic balance (Shimadzu, Libror AEU-210, Japan) that measured reproducibly within ± 0.0001 g.

X-ray Diffraction Analysis

X-ray diffraction (XRD) patterns were taken by using Ni-filtered Cuk_α radiation ($\lambda = 0.154$ nm) by X'pert diffractometer, Philips at 40 keV and 30 mA. The operating voltage and the current of the tube were kept the same throughout the investigation.

Differential Scanning Calorimetry Analysis

Thermograms on films were recorded using a Q10 model TA instrument to determine the glass transition temperature. The heating rate used was 10°C/min and the purge gas was nitrogen. The samples were analyzed from -50°C to 200°C.

Positron Annihilation Lifetime Spectroscopic Analysis

Positron annihilation lifetime spectra (PALS) is used to examine the free volume present in EVA samples. The Positron Lifetime Spectrometer consists of a fast-fast coincidence system with BaF_2 scintillators coupled to photo multiplier tubes type XP2020/Q with quartz window as detectors. The detectors were conical-shaped to achieve better time resolution. A17 mCi ^{22}Na positron source, deposited on a pure Kapton

foil of 0.0127 mm thickness, was placed between two identical pieces of the sample under investigation. This sample-source sandwich was positioned between the two detectors of PALS to acquire lifetime spectrum. The spectrometer measures 180 ps as the resolution function with ^{60}Co source.

However, for a better count rate, the spectrometer was operated at 220 ps time resolution [21]. All lifetime measurements were performed at room temperature and two to three positron lifetime spectra with more than a million counts under each spectrum were recorded. In PALS analysis there are two measured parameters, namely o-P_s lifetime (τ_3) and o-P_s intensity I_3. The o-P_s lifetime τ_3 measures the size of the free volume holes (V_f) and I_3 is a relative measure of the number of free volume sites in the polymer matrix.

The free volume cavity radius (R) is related to the o-P_s pick-off lifetime (τ_3) by a simple relation. The underlying assumption in the formulation of this relation is that o-P_s atom in a free volume cell can be approximated to a particle in a potential well of radius R_0. The potential is infinite if $r > R_0$ and constant for $r \leq R_0$. Further, it is assumed that there is an electron layer in the region $R < r < R_0$, with $R_0 = R + \delta R$ where δR represents the thickness of the electron layer or the probability of overlapping of the P_s wave function and electron wave function. The expression connecting the free volume radius R (in nm) and the o-P_s pick-off lifetime τ_3 (in ns) according to Nakanishi et al. [22] is

$$\left(\frac{1}{\tau_3}\right) = 2\left(1 - \left(\frac{R}{R_0}\right) + \left(\frac{1}{2\pi}\right)\sin\left(\frac{2\pi R}{R_0}\right)\right) \quad (1)$$

Here, the value of $\delta R = 0.1656$ nm was determined by fitting experimental τ_3 values to data from molecular materials with a well-known hole size, like zeolites. Using this value of R, the free volume size (V_f) is calculated as $V_f = (4/3)\,\pi R^3$. Then the relative fractional free volume is evaluated as the product of free volume (V_f) and o-P_s intensity, I_3 (%).

RESULTS AND DISCUSSIONS

Positron Annihilation Lifetime Spectroscopic (PALS) Analysis

An understanding of the free volume of polymers is crucial for determining their permeability and ionic conductivity. Today, PALS analysis is carried out for the experimental quantification of free volume [23,24]. It has been found that the estimated hole size significantly relates to the free volume property of polymer materials. Ito et al. [25] examined the relationship between the oxygen permeability

TABLE 2 PALS Measurements Data of EVA Samples

Sample	o-P_s lifetime, $\tau_3 \pm 0.01$ ns	o-P_s intensity $I_3 \pm 0.1\%$	Relative fractional free volume (F_v) %
D_0	2.35	15.9	3.78
D_1	2.33	20.48	4.78
D_2	2.37	15.08	3.63
D_4	2.34	14.53	3.42
D_6	2.34	13.04	3.06
D_8	2.35	12.6	2.2
B_1	2.33	25.06	5.85

and the free volume for ethylene-vinyl alcohol copolymer, which significantly followed the free volume theory as the ethylene content varied. The results obtained by them suggest that the molecular mechanism of gas permeation could be considered on the basis of local motion of the polymer segments and free volume size. Nagel et al. [26] correlated the free volume and transport properties of highly selective polymer membranes. Free volume values obtained for various EVA samples are given in Table 2.

From the table, it is inferred that the uncrosslinked sample (D_0) exhibits a low relative fractional free volume percentage compared to B_1 and D_1. Uncrosslinked EVA is a semicrystalline polymer. The crystalline regions account for the low free volume in the matrix since the chains are closely packed. When crosslinked by BP or DCP, the crystallinity is reduced due to the presence of random C-C crosslinks and the free volume increases. DCP-cured samples exhibited lower free volume percentage value than B_1. The explanation for this is that at the same loading of DCP or BP, more crosslinks were generated by DCP. The free volume decreases because the number of crosslinks increase. Hence DCP-cured samples exhibited lower free volume percentage values. Among the various DCP crosslinked samples, free volume percentage decreases from D_1 to D_8. As the amount of DCP increases, the number of crosslinks per unit volume increases and hence the free volume decreases.

Gas Permeation through EVA Membranes

The gas transport properties of uncrosslinked and crosslinked EVA samples have been analyzed using oxygen and nitrogen gases. The oxygen and nitrogen gas permeability coefficient of EVA membranes are shown in Figure 1(a) and (b), respectively. It is apparent from

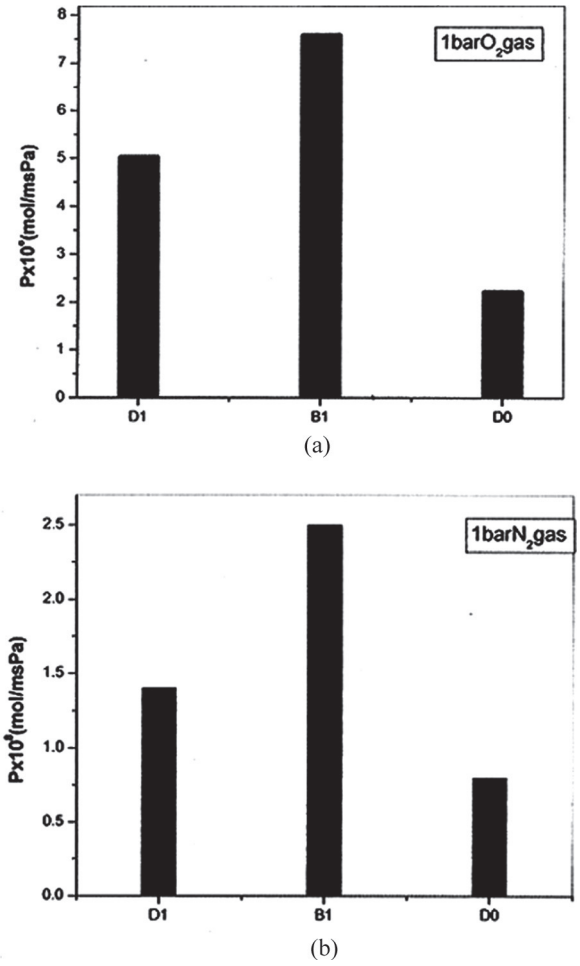

FIGURE 1 (a) Permeability coefficient of oxygen gas through EVA samples; (b) Permeability coefficient of nitrogen gas through EVA samples.

the figure that the uncrosslinked membranes showed the least permeability coefficient value. Poly(ethylene-co-vinyl acetate) is a semicrystalline polymer and the compact crystalline regions do not allow the permeation of gases. The presence of crystalline regions generate a more tortuous path for the penetrants to travel through the membrane. The sharp intense peak in the X-ray diffraction pattern given in Figure 2 supports the above observation. PALS results given in Table 2 show that the uncrosslinked EVA sample possessed a relatively lower fractional free volume percentage. Since the chain

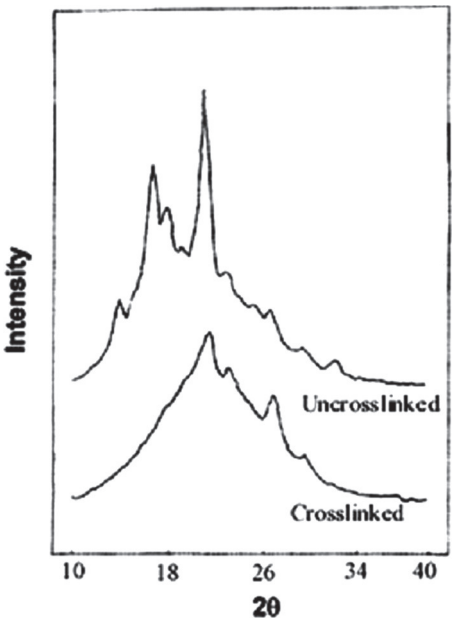

FIGURE 2 X-ray diffraction patterns of uncrosslinked and crosslinked membranes.

segments are closely packed in the crystalline part of the uncrosslinked sample, free volume decreases and as a result the gas permeability coefficient reduces.

The lightly crosslinked samples (D_1 and B_1) showed the highest values for gas permeation. When EVA was crosslinked by DCP or BP, the crystallinity was reduced due to the formation of C-C networks. The above situation is schematically represented in Figure 3. The porosity of the polymer is increased by the presence of moderate amounts of DCP or BP. When the crystalline fraction of the polymer decreases, there is an increase in the volume of amorphous fraction and chain lengths that connect the crystalline domains. A higher material volume accessible for gas sorption and higher flexibility of the network allow one to predict an increased transport of gases and higher permeation. The reduction in crystallinity is supported by the X-ray diffraction patterns. Modified membrane showed smaller peaks than unmodified one. PALS results given in Table 2 show that the free volume of the uncrosslinked polymer increases on the addition of DCP or BP.

Figure 1(a) and (b) also shows that BP crosslinked sample exhibits an increase in gas permeation compared to the DCP crosslinked

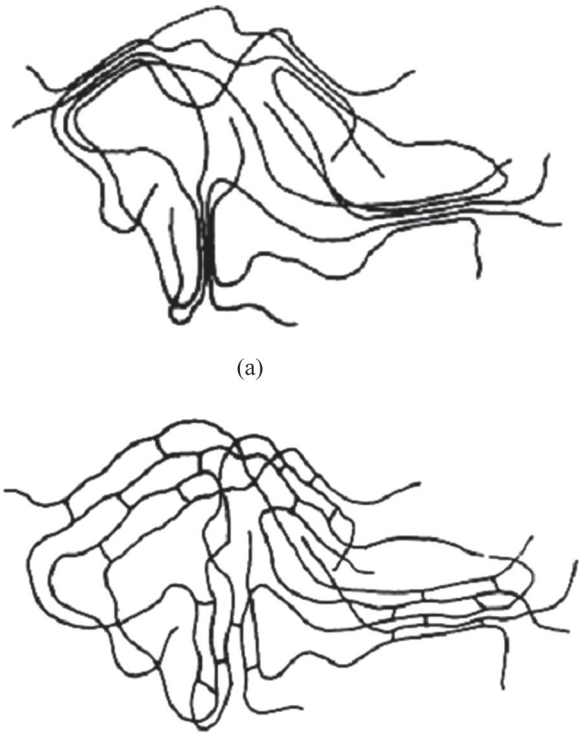

FIGURE 3 Schematic representation of the morphology of (a) Uncrosslinked (b) Crosslinked.

sample. The decrease in permeation is explained by the presence of more crosslinks generated by DCP than by BP, making it more difficult for the molecules to penetrate through the tightly crosslinked system.

PALS experiments (Table 2) also complement the gas permeation behavior of DCP and BP crosslinked samples. The table shows that the fractional free volume percentage (F_v%) is maximum for the B_1 system. The decrease in F_v for D_1 system is due to its high crosslink density.

Crosslink Density Measurements

The crosslink density of DCP and BP samples were determined by the equilibrium swelling method using benzene. The crosslink density

values give a clear picture of the different permeation behavior of crosslinked samples. The crosslink density (ν) is calculated using the equation

$$\nu = \frac{1}{2M_c} \tag{2}$$

where M_c is the molecular weight of the polymer between crosslinks. M_c is calculated using the equation [27]:

$$M_c = \frac{-\rho_p V \phi^{1/3}}{\ln(1-\phi) + \phi + \chi\phi^2} \tag{3}$$

where ρ_p is the density of the polymer, V is the molar volume of the solvent, ϕ is the volume fraction of the polymer in the fully swollen state and χ is the polymer–solvent interaction parameter. The volume fraction of the polymer is given by the equation [28]

$$\phi = \frac{w_1/\rho_1}{w_1/\rho_1 + w_2/\rho_2} \tag{4}$$

where w_1 and ρ_1 are the weight and density of the polymer and w_2 and ρ_2 are the weight and density of the solvent, respectively.

The polymer–solvent interaction parameter (χ) has been estimated from the equation [29]

$$\chi = \frac{(d\phi/dT)\{[\phi/(1-\phi)] + N\ln(1-\phi) + N\phi)\}}{2\phi(d\phi/dT) - \phi^2 N(d\phi/dT) - \phi^2/T} \tag{5}$$

N is calculated using the equation

$$N = \frac{[\phi^{2/3}/3 - 2/3]}{[\phi^{1/3} - 2\phi/3]} \tag{6}$$

DCP crosslinked sample showed a lower swelling in benzene than BP sample. The lower swelling is due to the higher crosslink density. The calculated values of crosslink density of B_1 and D_1 sample are 1.02×10^{-5} and 2.9×10^{-5} mol/cc respectively. In the present case, the amount of solvent absorbed by the D_1 sample decreases and hence the ϕ value increases leading to higher crosslink density. The increase in crosslink density suggests that the maximum number of crosslinks-per-unit volume is possessed by DCP vulcanized sample. Higher crosslink density values mean more restraint on the network and this results in lower swelling.

Differential Scanning Calorimetry Analysis

The differences in the crosslink density of DCP and BP crosslinked samples were also supported by the thermograms. Differential scanning thermograms of DCP and BP-cured EVA samples are depicted in Figure 4(a) and (b). It is seen that T_g and T_m of BP-cured EVA samples is -13.2° and 80.3°C, respectively. The decrease in the T_g of the BP-treated sample compared to the virgin sample is associated with the increase in amorphous content due to random crosslinking.

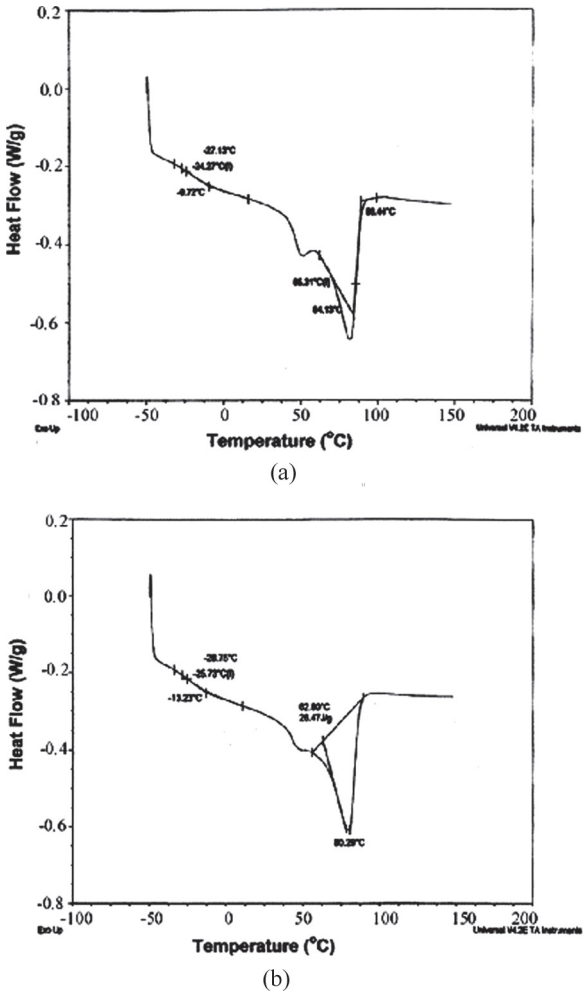

FIGURE 4 (a) Thermogram of D_1 sample; (b) Thermogram of B_1 sample.

The lower value of T_m is ascribed to the reduction in crystallinity of BP-treated EVA compared to the gum sample. Figure 4(a) reveals that the DCP-cured sample is having higher T_g than BP-cured EVA. This shows that the DCP-cured sample possessed higher crosslink density.

The glass transition temperature is an important factor controlling the transport process. As gas molecules pass through the polymer membrane, the rate of permeation is higher if the molecular structure is not rigid or the polymer has a high free volume. That is, the polymer having lower T_g has higher gas permeability. As the T_g decreases the gas permeability increases. Hence the high permeability of BP crosslinked sample is associated with its low glass transition temperature.

Selectivity of EVA Membranes

The polymeric membranes used for gas separation processes have properties such as high permeability to the desired gas, high selectivity and the ability to form useful membrane configurations. The requirement of an ideal membrane is high permeability together with high permselectivity. The permselectivity of a membrane is given by

$$\alpha(O_2, N_2) = \frac{P(O_2)}{P(N_2)} \tag{7}$$

where, α is the permselectivity of a membrane towards O_2 and N_2 gas $P(O_2)$ and $P(N_2)$ are the permeability constants of O_2 and N_2 gases, respectively.

The variation of selectivity with crosslinking systems is shown in Figure 5. It is clear from the figure that DCP-modified membrane exhibits higher selectivity than BP-modified membrane. The sample which exhibits higher permeability shows low selectivity and vice versa. The observed selectivity is also related to the crosslink density of the samples. As the gas molecules pass through polymer chains, the rate of permeation is higher if the molecular structure is flexible or the polymer has a high free volume. The observed change in permeability of the two membranes is due to the variation in the flexibility of the networks resulting from the different degrees of crosslinking.

Effect of the Amount of Crosslinker

The permeability coefficients of DCP-crosslinked EVA membranes are shown in Figure 6. It can be seen that the oxygen permeability decreases as the amount of DCP increases. This behavior is associated with the increase in crosslink density. The decreased gas permeability

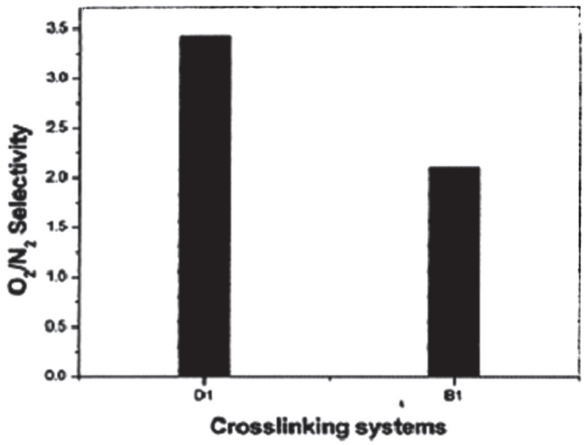

FIGURE 5 Variation of selectivity with crosslinking systems.

is due to the tortuous path generated by the crosslink networks. The above results are complemented by PLAS measurements of fractional free volume percentage (Table 2). It can be seen that the free volume decreases from D_1 to D_8. When more and more crosslinks are formed, the available free volume decreases, resulting in a reduced gas permeability. The D_8 system with the highest crosslink density exhibits the lowest gas permeability.

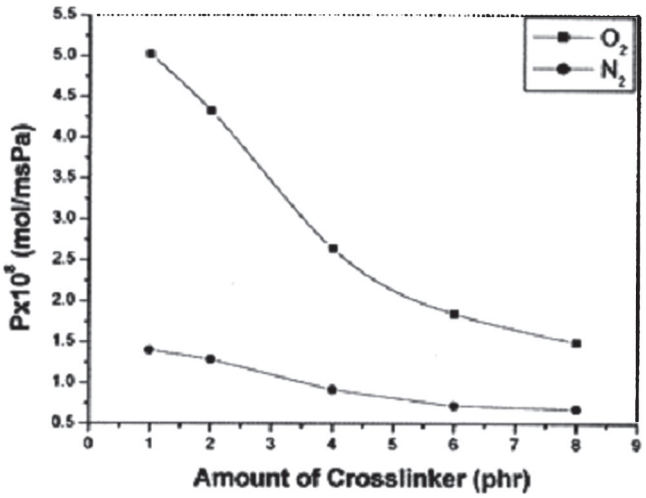

FIGURE 6 Influence of the amount of crosslinker on permeability.

The effect of penetrant size on the diffusion of gas molecules through these membranes can also be understood from Figure 6. As compared to nitrogen, oxygen has more permeability due to the lower covalent radius of oxygen. This can be explained by using the Stoke-Einstein equation; according to them the diffusion of gas molecules is inversely related to the friction exerted. The equation is given by

$$\mathrm{D} = \frac{k_B T}{f} \tag{8}$$

where k_B is the Boltzmann constant, T is the absolute temperature and f is the friction factor. As the radius of the gas molecule increases the friction factor also increases by the relation,

$$\mathrm{F} = 6\pi\mu\mathrm{R}_0 \tag{9}$$

and thereby the permeability decreases. Here, π is the viscosity of the solvent and R_0 is the radius of the diffusing gas molecule.

The permeabilities of polymer appear to be a very sensitive function of penetrant size. Figure 6 shows that oxygen exhibits higher permeability compared to nitrogen. This is due to the increase in the covalent radius of nitrogen.

CONCLUSIONS

The gas transport characteristics of uncrosslinked and crosslinked poly(ethylene-co-vinyl acetate) membranes were investigated using nitrogen and oxygen gases. Due to the tortuous path generated by crystalline domains, the uncrosslinked EVA sample exhibited lower permeability to these gases. The higher permeability of crosslinked samples is associated with the increase in the free volume of the polymer matrix. Benzoyl peroxide lightly crosslinked membranes exhibited higher oxygen permeability than the dicumyl peroxide system. The free volume of the DCP-crosslinked sample is lower than that of the BP-crosslinked sample because of its high crosslink density. The higher crosslink density accounts for the lower permeation of gases through DCP-crosslinked sample. The crosslink density was computed by equilibrium swelling method and the values support the permeation behavior. The size of the penetrant gas molecule affects the permeability coefficient. The covalent radius of the nitrogen gas molecule is larger than the oxygen gas molecule, and hence nitrogen shows reduced permeability. From the plots of permeability against the amount of crosslinker it was found that the gas permeability decreased with increased crosslink density. Finally, it is important

to add that glass transition temperature measurement and positron annihilation lifetime spectroscopic analysis complement the gas permeation behavior.

REFERENCES

[1] Patricio, P. S. O., De Sales, J. A., Silva, G. G., Windmoller, D., and Marchado, J. C., *J. Membr Sci.* **271**, 177 (2006).
[2] Scheichl, R., Klopffer, M. H., Benzellonn-Dahaghi, Z., and Flaconneche, B., *J. Membr. Sci.* **254**, 275 (2005).
[3] Jiang, L. Y., Chung, T. S., and Kulprathipanja, S., *J. Membr. Sci.* **276**, 113 (2006).
[4] Fu, Y. J., Hu, C. C., Lee, K. R., Tsai, H. A., Ruaan, R. C., and Lai, J. Y., *Eur. Polym. J.* **43**, 959 (2007).
[5] Toi, K., Morel, G., and Paul, D. R., *J. Appl. Polym. Sci.* **27**, 2997 (1982).
[6] Chern, R. T., Shes, F. R., Jion, L., Stannett, V. T., and Hopfenberf, H. B., *J. Membr. Sci.* **35**, 103 (1987).
[7] Chiou, J. C., Maede, Y., and Paul, D. R., *J. Appl. Polym. Sci.* **35**, 1823 (1987).
[8] Min, K. E. and Paul, D. R., *J. Polym. Sci. Part B: Phys.* **26**, 1021 (1988).
[9] Ichiraku, Y., Stern, S. S., and Nakagawa, T., *J. Membr. Sci.* **34**, 5 (1987).
[10] Compan, V., Zanuy, D., Andrio, A., Morillo, M., Aleman, C., and Guerra, S. M., *Macromolecules* **35**, 4521 (2002).
[11] Arnold, M. E., Nagai, K., Freeman, B., and Spontak, J. R., *Macromolecules* **34**, 5611 (2001).
[12] Naylor, T. (1989). *Hand Book of Comprehensive Polymer Science*, Pergamon Press, UK.
[13] Pixton, M. R. and Paul, D. R., *Macromolecules* **28**, 8277 (1995).
[14] Aitken, C. L., Koros, W. J., and Paul, D. R., *Macromolecules* **25**, 3651 (1992).
[15] Tiemblo, P., Guzman, J., Riande, E., Mijangos, C., and Reinecke, H., *Macromolecules* **35**, 420 (2002).
[16] Sridhar, S., Suryamurali, R., Smitha, B., and Aminabhavi, T. M., *Colloids and Surfaces A: Physicochemical and Engineering Aspects* **297**, 267 (2007).
[17] Van Amerongen, G. J., *J. Appl. Phys.* **17**, 972 (1946).
[18] Johnson, T. and Thomas, S., *Polymer* **40**, 7511 (1999).
[19] George, S. C., Ninan, K. N., and Thomas, S., *Eur. Polym. J.* **37**, 183 (2001).
[20] Chen, S. H., Ruaan, R. C., and Lai, J. Y., *J. Membr. Sci.* **134**, 143 (1997).
[21] Ravikumar, H. B., Ranganathaiah, C., Kumaraswamy, G. N., and Thomas, S., *Polymer* **46**, 2372 (2005).
[22] Nakanishi, H., Jean, Y. C., Schrader, D. M., and Jean, Y. C., Eds. (1988). *Positron and Positronium Chemistry*, Elsevier, Amsterdam p. 159.
[23] Tanaka, K., Kawai, T., Kita, H., Okamoto, K., and Ito, Y., *Macromolecules* **33**, 5513 (2000).
[24] Kobayashi, Y., Haraya, K., Hattori, S., and Sasuga, T., *Polymer* **35**, 925 (1994).
[25] Ito, K., Saito, Y., Yamamoto, T., Ujihira, Y., and Nomura, K., *Macromolecules* **34**, 6153 (2001).
[26] Nagel, C., Gunther-Schade, K., Fritsch, D., Strunskus, T., and Faupel, F., *Macromolecules* **35**, 2071 (2002).
[27] Flory, P. J. and Rehner, J., *J. Chem. Phys.* **11**, 521 (1943).
[28] Cassidy, P. E., Aminabhavi, T. M., and Thompson, C. M., *Rubber Chem. Technol.* **56**, 594 (1983).
[29] Unnikrishnan, G. and Thomas, S., *Polymer* **35**, 25 (1994).